Enhancement of the Supercurrent at a Finite Voltage in a Sandwich-Type Ballistic SINIS Junction

I. P. Nevirkovets,[1,2] S. E. Shafranjuk,[1] O. Chernyashevskyy,[1,2] and J. B. Ketterson[1,3]

[1]*Department of Physics and Astronomy, Northwestern University, Evanston, Illinois 60208, USA*

[2]*Institute for Metal Physics NASU, 03680 Kyïv, Ukraine*

[3]*Department of Electrical Engineering and Computer Science, and Materials Research Center, Northwestern University, Evanston, Illinois 60208, USA*

(Received 14 September 2006; published 19 March 2007)

A large, reentrant, Josephson current is observed in SINIS (Nb/Al/AlO_x/Al/AlO_x/Al/Nb) junctions at a finite voltage close to Δ/e (where Δ is the superconducting energy gap in S) and a bias current exceeding the zero-voltage Josephson current. The effect is studied using a multiterminal device configuration. A theoretical interpretation in terms of quantized electron states in the N layer is provided.

DOI: 10.1103/PhysRevLett.98.127002 PACS numbers: 74.45.+c, 74.50.+r, 74.78.Fk, 85.25.Am

In the past, enhancements of the superconducting critical current in weakly coupled superconducting systems were reported for experimental situations where the quasiparticle distribution function in a superconductor was driven out of equilibrium [1,2]. In the past few decades, it was realized that superconducting bound states play the crucial role in Josephson tunneling [3,4]. By manipulating the population of the bound states, it is possible to greatly enhance the Josephson current as compared with its equilibrium value [5]. In the case of ballistic SNS [3] or SINIS [6,7] junctions, Andreev bound states (ABS) [8] in the normal layer govern the supercurrent transfer (here S, I, and N denote a superconductor, an insulator, and a normal metal, respectively). An enhancement of the supercurrent at finite voltage in SNS junctions (with N being a two-dimensional electron gas) by microwave irradiation, interpreted as the introduction of a nonequilibrium ABS quasiparticle population, was demonstrated experimentally by Lehnert *et al.* [9].

In this Letter, we report an extreme reentrant enhancement of a Josephson current in ballistic SINIS (Nb/Al/AlO_x/Al/AlO_x/Al/Nb) junctions without any external perturbation, studied using a multiterminal geometry [10]. The effect of the enhancement of the Josephson current manifests itself as a steplike structure at a finite voltage, mimicking the zero-voltage Josephson critical current, but which is observed in a narrow interval close to Δ/e; the current amplitude of the anomalous feature can exceed the magnitude of the conventional zero-voltage Josephson critical current I_c and appear at a bias current above I_c (reentrant behavior). Our former experiments [7] were indirect in the sense that the SINIS junction was a two-terminal device, and, hence, it was not possible to determine the state (superconducting or resistive) of each (SIN and NIS) interface while biasing the junction at a voltage where the anomalous feature appeared; one might then speculate that the feature was due to a short-circuiting of one of the interfacial junctions or due to a superconducting transition of the N layer. Using the multiterminal geometry, we can now firmly establish that the anomalous Josephson current is a novel feature intrinsic to SINIS junctions. We also present a theoretical interpretation of the observed phenomenon in terms of ABS formation in the SINIS "quantum box."

Our multilayer Nb/Al/AlO_x/Al/AlO_x/Al/Nb structure was *in situ* fabricated as described elsewhere [10]. A schematic cross-sectional view of the multiterminal device is shown in Fig. 1(a). Here we describe devices with a width $W = 10\ \mu$m and lengths $L_b = 19\ \mu$m and $L_t = 11\ \mu$m for the bottom and top junctions, respectively. The specific tunneling resistance of the barriers was of the order of $1 \times 10^{-7}\ \Omega \times \mathrm{cm}^2$, which, by technological measures, means high-transparency junctions but physically corresponds to a rather low tunneling probability $D \sim 10^{-4}$–10^{-5}. The thickness of the middle Al layer d_N was varied from 7 to 20 nm, so that $d_N \leq l$, where l is the

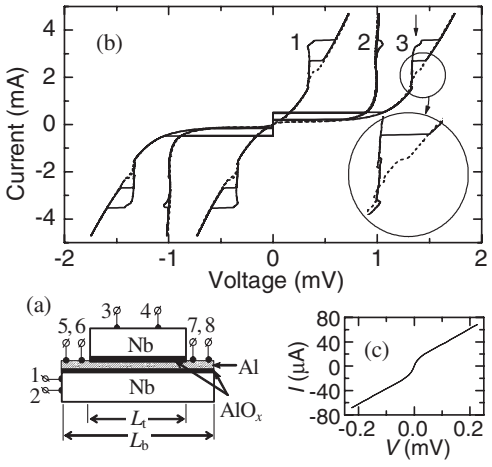

FIG. 1. (a) Schematic cross-sectional view of the multiterminal SINIS device. (b) Solid lines: CVCs of a SINIS device at 1.8 K when feeding the current between terminals 1 and 3 and measuring the voltage between terminals 5 and 4 (curve 1), 2 and 5 (curve 2), and 2 and 4 (curve 3). Dashed lines: The same curves measured in an applied magnetic field of 220 Oe. Inset: Blowup of an initial portion of an anomalous step (marked by a vertical arrow). (c) The initial portion of the CVC of the N layer measured between terminals 5 and 8 (for current) and 6 and 7 (for voltage).

electron mean free path (being at least 20 nm at low temperatures, as estimated from resistivity measurements of similar Al films).

First, we consider the current-voltage characteristics (CVCs) of a multiterminal Nb/Al/AlO_x/Al/AlO_x/Al/Nb device with $d_N = 13$ nm (device 1) at 1.8 K, where both the zero-voltage Josephson current and an anomalous feature at $V \approx \Delta/e$ are observed. Figure 1(b) shows the CVC of this device recorded while feeding the current between terminals 1 and 3 and measuring the voltage between terminals 5 and 4 (curve 1), 2 and 5 (curve 2), and 2 and 4 (curve 3). Curve 3 represents the SINIS device as whole, while curves 1 and 2 are CVCs of the top and bottom junctions, respectively. The feature of interest, appearing in curve 3 at $V \approx \Delta/e$ (marked by a vertical arrow), has the same shape as that for two-terminal junctions that were fabricated on the same substrate, so the multiterminal geometry does not affect the physical processes leading to the step formation. Algebraic summation of curves 1 and 2 exactly reproduces curve 3. From a comparison of the Josephson critical current densities in the two- and multiterminal devices, we conclude that, in the latter case, the current flows perpendicular to the layers within the area defined by the top Nb electrode. It is clear from the curves in Fig. 1(b) that the feature of interest is ''divided'' between the top and bottom junctions so that it appears at $V \approx \Delta/4e$ in the CVC of the top junction, where it is more pronounced than in the bottom junction. These features are magnetic-field-dependent for both junctions; in Fig. 1(b), the same curves are shown in a magnetic field of 220 Oe applied parallel to the layers (dashed lines). It is important that the features appear in the CVCs of the top and bottom junctions at finite (nonzero) voltage, and, therefore, the resultant feature seen in the CVC of the whole SINIS device is not due to a superconducting short or a dc Josephson current in one of the constituent junctions but is related to a peculiarity in the tunneling density of states. The CVC of the N layer [cf. Fig. 1(c)] measured in the lateral direction (using terminals 5 and 8 for the current and 6 and 7 for the voltage) indicates that, within the resolution of our measurement technique (1 μA), the layer is dissipative, although, at the same time, a zero-voltage supercurrent of about 0.5 mA can flow perpendicular to the layers.

It is interesting to study the response of the N layer to a current injected perpendicular to the layers, particularly in the region where the Josephson current through the SINIS device appears at a finite voltage $V \approx \Delta/e$, constituting the anomalous feature. Figure 2 shows a family of CVCs of the N layer of another SINIS device with $d_N = 16$ nm (device 2) at various injection levels $I_{inj} = \pm 4, \pm 3, \pm 2$, and 0 mA perpendicular to the SINIS structure at 1.8 K in both zero magnetic field and in a magnetic field of 52 Oe applied parallel to the layers; I_{inj} levels are indicated by arrows in the lower inset in Fig. 2, where a portion of the CVC of

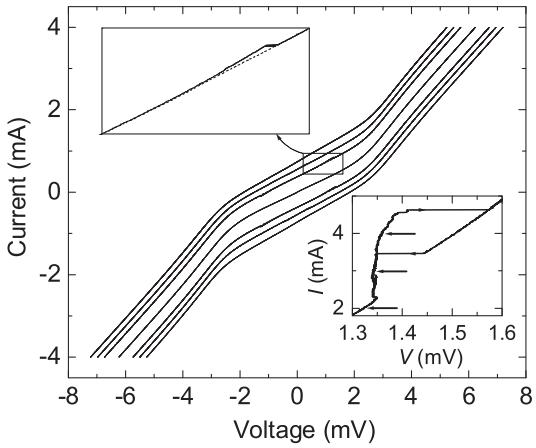

FIG. 2. A family of CVCs of the middle Al layer in a Nb/Al/AlO_x/Al/AlO_x/Al/Nb device at 1.8 K for various injection levels across the layers. Curves from top to bottom are for $I_{inj} = +4, +3, +2, 0, -2, -3$, and -4 mA, respectively. The upper inset is a blowup of a portion of the CVC for $I_{inj} = +2$ mA showing the presence of the coherent current (the solid line is for $H = 0$, and the dashed line is for $H = 52$ Oe). Lower inset: A portion of the CVC of the same device showing an anomalous step; injection levels $I_{inj} = +2, +3$, and $+4$ mA are marked by arrows.

device 2, displaying the anomalous current step in the perpendicular characteristics, is shown. Here the ''+'' direction corresponds to the current flowing from terminal 3 to terminal 1 [cf. Fig. 1(a)]. As the injection current increases from zero, a magnetic-field-sensitive feature appears in the CVC of the N layer; the amplitude of this ''coherent'' current originally increases but then decreases and is not resolved for $I_{inj} > 3$ mA. A portion of the CVC for $I_{inj} = +2$ mA is shown on a magnified scale in the upper inset in Fig. 2 (the solid curve is for $H = 0$, and the dashed curve is for $H = 52$ Oe). The appearance of the coherent current in the CVC of the N film for $I_{inj} > 0$ indicates injection of superconducting electrons from S to N, an effect interesting in its own right.

Since the anomalous step in the CVC of the SINIS device corresponds to I_{inj} between 2.3 and 4.7 mA, we conclude that the appearance of the anomalous Josephson (AJ) current has no detectable influence on the lateral conductivity of the N layer. It would therefore appear that the AJ current is dominated by electrons with momenta perpendicular to the layers.

In Fig. 3, we show a detailed dependence of the amplitude of the magnetic-field-sensitive current I_s associated with the AJ effect for the device 1 at 2.1 (triangles) and 3.9 K (open squares). The current I_s was measured with a voltage criteria of 50 μV (i.e., the width of the step was assumed to be 50 μV) at 2.1 K and with a voltage criteria of 20 μV at 3.9 K (the step structure was situated within a narrower voltage interval at higher temperature). Note the complicated shape of the $I_s(H)$ dependence, which can

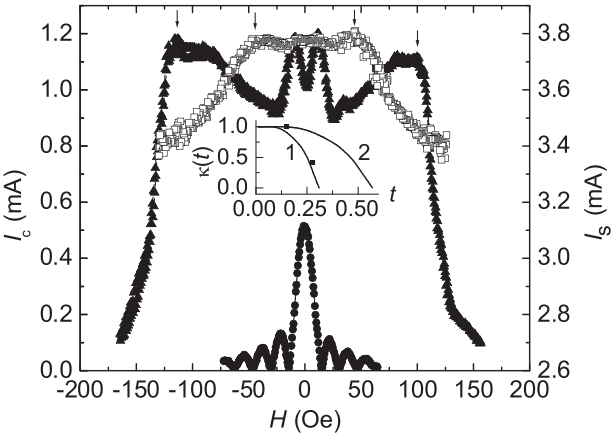

FIG. 3. $I_s(H)$ and $I_c(H)$ dependences of a Nb/Al/AlO_x/Al/AlO_x/Al/Nb device (cf. Fig. 1). Triangles and open squares: $I_s(H)$ dependence at 2.1 and 3.9 K, respectively; circles: $I_c(H)$ dependence at 1.8 K. The inset shows the dependence of the reduced period $\kappa(t) = \lambda_L(0)/\lambda_L(T)$ of the Fraunhofer pattern versus the reduced temperature $t = T/\Delta(0)$. Curve 1 is the theoretical fit using this approach [7,12]; curve 2 is the corresponding equilibrium dependence. Squares correspond to experimental dependences shown in the main panel (see explanation in the text).

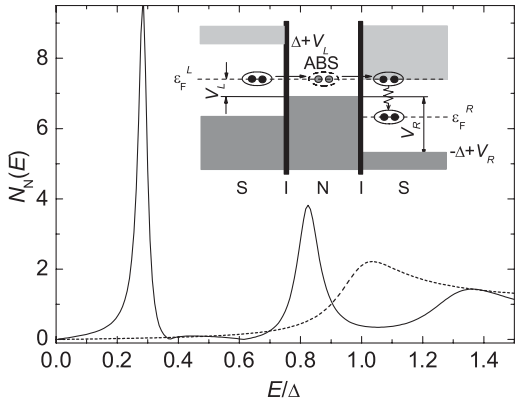

FIG. 4. Single-electron density of states inside of the middle N layer of a SINIS junction for $d_N = 1.46\xi_{\mathrm{BCS}}$ (solid line). Dashed line: The corresponding BCS curve for a SIS junction. The inset shows elementary processes contributing to the anomalous Josephson supercurrent.

vary for specimens with different parameters (e.g., barrier transparency and thickness of the middle N layer). A typical feature of the $I_s(H)$ dependence is minimum at $H = 0$ [7]. The shape of the $I_s(H)$ dependence alters sensitively with temperature [unlike the $I_c(H)$ diffraction pattern (shown in Fig. 3 by circles), whose period is almost constant in the same temperature range]; this behavior can be explained within our theoretical model outlined below.

The observed dc AJ effect can be interpreted in terms of the quantized ABS states formed inside the middle N layer. In SINIS junctions, the ABS levels are much sharper than the BCS singularity, and their positions do not coincide with $E = \pm\Delta$; this allows for the ABS identification. A finite bias voltage, applied across the SINIS junction, drops almost entirely on the insulating barriers; thus, the electric field inside the N layer is negligibly small. This ensures that the quantization condition for ABS formation in N is fulfilled (unlike the case of a SNS junction). According to Refs. [3,4,8,11,12], the ABS energy bands $E_n(\varphi_1, \varphi_2)$ of a "clean" SINIS junction depend on the phase differences φ_1 and φ_2 across the left and right barriers (see schematic of the tunneling process in the inset in Fig. 4). The detailed band structure depends on the thickness of the middle layer and on the junction transparency [12]. Since the transparency of our junction is relatively low, the energy bands are very narrow, i.e., $E_n(\varphi_1, \varphi_2) \simeq E_n^0 + E_n^1(\varphi_1, \varphi_2)$, $E_n^0 \gg E_n^1(\varphi_1, \varphi_2)$. The last condition allows for studying the ABS levels by injecting into them phase-coherent pairs of charge carriers and quasiparticles at a finite dc voltage applied across the junction. The ground state of the junction is defined as a symmetric combination $|0_s\rangle = (|0_+\rangle + |0_-\rangle)/\sqrt{2}$ of the corresponding eigenfunctions $|0_+\rangle$ and $|0_-\rangle$, which actually corresponds to a ground state energy $E_s = E_+ + E_- = 0$. The steady state of the junction is related to the state $|0_s\rangle$, associated also with a dc Josephson supercurrent transferred by Cooper pairs (CP). The magnitude of the microscopic conventional dc Josephson (CJ) supercurrent is obtained as $I_s(\varphi) = I_s^+ + I_s^- = 2(2\pi/\Phi_0)(\partial E_+^1(\varphi)/\partial\varphi)$, where Φ_0 is the flux quantum. For $V \neq 0$ and $V < \Delta/e$, the conventional ac Josephson effect takes place.

The symmetric wave function $|0_s\rangle$ should generally be accompanied by an antisymmetric combination $|0_{\mathrm{as}}\rangle = (|0_+\rangle - |0_-\rangle)/\sqrt{2}$, with a corresponding finite-energy eigenvalue $2E_a = E_+(\varphi) - E_-(\varphi) = 2[E^0 + E^1(\varphi)] \neq 0$ interpreted as a finite energy (measured from the Fermi energy ε_F^N of the N layer) acquired by CP upon transfer across the junction in a phase-coherent process where both the electron $[E_+(\varphi)]$ and hole $[E_-(\varphi)]$ energies are positive. The dc AJ current starts to flow for a bias voltage $V \approx \Delta/e$ across the whole SINIS junction, as shown schematically in the inset in Fig. 4. Some fraction of all phase-coherent electrons (participating in the transport) cross the N layer ballistically via the ABS level and then tunnel into the excited CP state that extends deeply into the right S electrode (on a distance $\sim 10\xi_{\mathrm{BCS}}$ [7,12], where ξ_{BCS} is the BCS coherence length); these *noneqilibrium* CPs [13] contribute to the dc AJ effect and form a near-vertical step for $V \approx \Delta/e$ in the CVC.

At the resonance leading to AJ, the CP energy in the left S electrode $E_{\mathrm{CP}}^L = 2eV_L$ matches the energy of an ABS level in the N layer $E_{\mathrm{ABS}} = 2E_a$, which gives $V_L = E_a/e$. By matching the ABS energy E_{ABS} with the CP energy in the right S layer $E_{\mathrm{CP}}^R = 2\Delta - 2eV_R$, one obtains $V_R = (\Delta - E_a)/e$. (Here we assume that the N layer is at zero potential.) Thus, the net voltage drop across the whole SINIS junction at the resonance is $V_L + V_R = \Delta/e$ (re-

gardless of the E_a magnitude), which agrees with our experimental observation. If $V > \Delta/e$, we predict an ac AJ effect with a frequency $\omega_A = 2(eV - \Delta)/\hbar$ (in addition to the ac CJ radiation frequency $\omega = 2eV/\hbar$). Another condition for the occurrence of the dc AJ supercurrent is that the CPs must reside at the finite energy $\varepsilon \approx \Delta$ (ε is measured from the Fermi energy of S) for a sufficiently long time $\tau_\varepsilon > d_N/v_F$, which means that the energy relaxation time τ_ε of the excited CPs into the superfluid condensate (i.e., to $\varepsilon = 0$) of the right S electrode must be sufficiently long. Since the quantization axis $\hat{x}$ is perpendicular to the junction plane, the supercurrent through the N layer is due purely to the ABS [3,4,8,11,12]. Such an ABS-carried supercurrent has a nonvanishing current only in the direction perpendicular to the junction plane, while the in-plane components vanish. This is fully consistent with our experimental observation of an enhanced supercurrent perpendicular to the N layer, while the current parallel to the N layer is dissipative.

The magnitude as well as the spatial distribution of the nonequilibrium dc AJ current deep in the S electrodes depend on the temperature, resulting in the temperature-dependent $I_s(H)$ pattern. This is illustrated in the inset in Fig. 3, where curve 1 is the theoretical dependence of the normalized period of the Fraunhofer pattern $\kappa(t) = \lambda_L(0)/\lambda_L(T)$ versus $t = T/\Delta(0)$, calculated using the approach [7,12] for the scenario described above (here λ_L is the magnetic-field penetration depth in S). The nonequilibrium penetration depth is given by $\lambda_L = (2/\pi) \times \int_0^\infty dq/[q^2 + 4\pi e^2 Q(q)/m]$, where the electromagnetic kernel is $Q(q) \approx 3\pi^2 n\Delta(1 - 2f_{\varepsilon=\Delta})/(4v_F q)$, and the nonequilibrium electron distribution function $f_{\varepsilon=\Delta}$ is obtained numerically [7,12]; here n is the concentration of normal electrons and v_F is the Fermi velocity. Curve 2 is the corresponding equilibrium dependence of $\kappa(t)$ [when defining $\kappa(t)$ as a period of the diffraction pattern, we neglect a contribution to the magnetic thickness of the barrier layer, which is much smaller than λ_L in real junctions]. As a measure of the period of the experimental Fraunhofer pattern, we assume the width between the main maxima in the $I_s(H)$ dependence, marked with the arrows. Then, normalizing this width to that measured at 2.1 K, we obtain two experimental points in the $\kappa(t)$ dependence (squares in the inset in Fig. 3). These points lie slightly above (but close to) the nonequilibrium curve 1, because the period at 2.1 K is smaller than the maximum period at lower temperatures; we therefore conclude that the theory describes the basic experiment behavior.

We also computed the single-electron density of states (DOS) using this approach [12]. The solid curve in Fig. 4 is for a low-transparency ($D \sim 10^{-4}$–10^{-5}) SINIS junction with $d_N = 1.46\xi_{\mathrm{BCS}}$. In calculations, d_N was used as a fitting parameter to obtain the main ABS peak at $E = \Delta/4$, which corresponds to the experimental observation [see curve 1 in Fig. 1(b)]. Since a typical value of ξ_{BCS} for sputter-deposited Nb films is about 10 nm, and $d_N =$ 13 nm in the experiment, the agreement between the theoretical and experimental d_N values can be regarded as reasonably good. The DOS is computed using a quasiclassical Green's function approach (see Refs. [4,11] and references therein). As can be seen from curve 1, in addition to a sharp ABS peak at $E = \Delta/4$, there is a much weaker ABS peak at $E = 3\Delta/4$. The dashed curve in Fig. 4 is the usual BCS density of states, with the singularity at $E = \Delta$ being much weaker than the ABS-related peaks.

In conclusion, we have observed the appearance of an anomalous Josephson current in SINIS devices at a finite voltage $V \approx \Delta/e$ and a bias current exceeding the zero-voltage Josephson current I_c; the amplitude of this anomalous current can be considerably higher than I_c. The anomalous current is related to the formation of Andreev bound states in the system.

The authors are thankful to E. Goldobin for using his GOLDEXI software. This work was supported by the National Science Foundation under Grants No. EIA-0218652 and No. DMR-0509357. One of the authors (S. S.) acknowledges support from AFOSR Grant No. FA9550-06-1-0366.

[1] A. F. G. Wyatt *et al.*, Phys. Rev. Lett. **16**, 1166 (1966).
[2] A. H. Dayem and J. J. Wiegand, Phys. Rev. **155**, 419 (1967).
[3] I. O. Kulik, Sov. Phys. JETP **30**, 944 (1970).
[4] A. Furusaki and M. Tsukada, Phys. Rev. B **43**, 10 164 (1991).
[5] G. Wendin and V. S. Shumeiko, Phys. Rev. B **53**, R6006 (1996).
[6] A. Brinkman and A. A. Golubov, Phys. Rev. B **61**, 11 297 (2000).
[7] I. P. Nevirkovets *et al.*, Phys. Lett. A **269**, 238 (2000); Phys. Rev. B **68**, 024514 (2003).
[8] A. F. Andreev, Sov. Phys. JETP **19**, 1228 (1964).
[9] K. W. Lehnert *et al.*, Phys. Rev. Lett. **82**, 1265 (1999).
[10] I. P. Nevirkovets *et al.*, J. Appl. Phys. **97**, 123903 (2005); Phys. Rev. Lett. **95**, 247008 (2005).
[11] C. W. J. Beenakker and H. van Houten, Phys. Rev. Lett. **66**, 3056 (1991).
[12] S. E. Shafranjuk and J. B. Ketterson, Phys. Rev. B **72**, 212506 (2005); **72**, 024509 (2005); S. E. Shafranjuk, Phys. Rev. B **74**, 024521 (2006).
[13] Although the standard BCS theory for a bulk, uniform superconductor does not imply a nonequilibrium CP population at $\varepsilon > 0$, the nonequilibrium population is possible in systems with Josephson coupling, as discussed theoretically by Rogovin and Scully [Phys. Rep. **25**, 175 (1976)] and observed experimentally by Barbara *et al.* [Phys. Rev. Lett. **82**, 1963 (1999)].